intertidal sand flats (Table 2). Lowstand deposits are high intertidal to supratidal shale (Table 2). At Mount Union, this fifth-order sequence consists entirely of red shale, probably of non-marine origin (Table 2).

Comparison of the interval with the model of a complete fifth-order sequence (Figure 7) suggests that PAC 1 is missing at all three localities owing to non-deposition (hiatus) prior to the initial deposition over (flooding of) the basal unconformity. Sequence II *A* is thicker, more complete, and more marine at the southern localities suggesting deposition on a gentle slope. Precession-driven sea-level rises flooded this sloping surface differentially, in steps. Presuming that the second sixth-order cycle is an augmented relative sea-level rise within the fifth-order sequence, then PAC 2 was deposited and preserved at all three localities. In that case, PACs 3, 4, and 5 at Mount Union were either not deposited (because subsequent sea-level rises did not reach that far landward), or cycle boundaries were obliterated by bioturbation. Comparable thicknesses at all three localities suggest that PACs 3, 4, and 5 were obscured at Mount Union (Appendix B).

Fifth-order Sequence II *B*

Fifth-order Sequence II *B* begins at a major facies change where the supratidal shales of the sequence below are overlain by low intertidal sandstones and carbonates (Figure 13 and Table 2). This predominantly sandstone sequence is complete (containing 5 PACs) at Pinto, MD and consists of 4 PACs at Mount Union. At Cedar Cliff, only two PACs were identified, but the similarity in thickness relative to Pinto suggests that some cycle boundaries could not be discerned at Cedar Cliff (Appendix B).

Figure 13. Sequence II *B* at Pinto, Maryland. Sequence II *B*, bounded by green lines, contains 5 PACs, which are delineated by white lines. PACs in this sequence are delineated by clay seams at non-depositional surfaces in bedded gray-brown sandstone. Measuring sticks are 4 feet long; stratigraphic up is to the left.

At the most complete section, Pinto, the cycles consist of subtidal, gray-brown laminated calcisiltite and sandstones (Table 2) that consist of moderately- to well-sorted carbonate or quartz grains averaging 0.1 mm in diameter (Figure 14). These marine sandstones at Pinto contrast with the iron-rich red sandstones containing poorly sorted grains of quartz (ranging from 0.1 mm to .01 mm), silt, and clay (Figure 15) at Mount Union. These differences in composition, grain size, sorting, and the presence of oxidized iron at Mount Union suggests that the depositional environments at the two localities were quite different. At the northern locality, the poorly sorted fine grained-clastics were deposited nearer to the clastic source, in a non-marine setting (Table 2), while Pinto was a shallow marine setting, where persistent current activity produced well-sorted deposits. At both localities, PACs are recognized by non-depositional surfaces marked by thin clay beds. Absence of these surfaces in Sequence II *B* at Cedar Cliff makes cycle definition problematic. However a paleosoil present at the top of the sequence indicates prolonged exposure (Appendix B). Sequence II *B* is anomalously thick at Mount Union (15 feet versus 10.5 feet at the southern localities).

Deposition of cycles in this sequence was controlled by position of each locality relative to the shoreline. The sea-level rise that initiated Sequence II *B* flooded the high intertidal shales terminating Sequence II *A* at Pinto, but did not flood the Mount Union area. The second sea-level rise, resulting in PAC 2, flooded all three localities. Eccentricity-dampened sea-level rises also flooded the entire region, resulting in PACs 3, 4, and 5. At Cedar Cliff, the presence of the paleosol at the top of PAC 3 was interpreted to form on a topographic high point, exposing the top of the sequence for the duration of

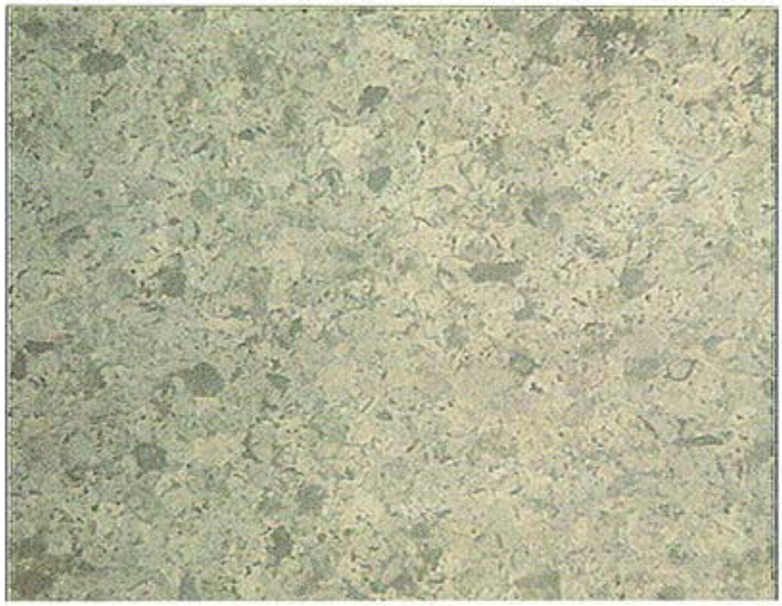

Figure 14. Thin Section of the Base of PAC 2, Sequence II *B* at Pinto, MD. The base of PAC 2 in Sequence II *B* consists of subrounded to rounded carbonate and quartz grains. The field of view is 1.4 mm horizontally.

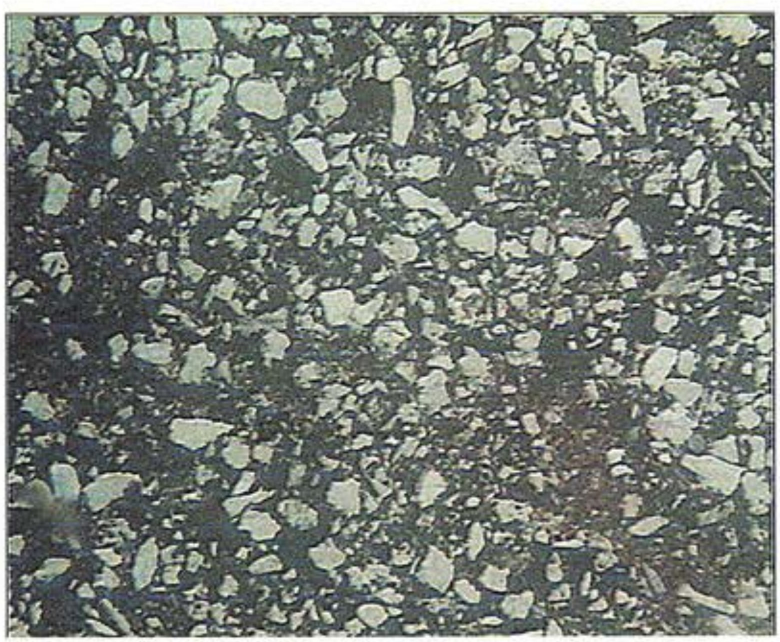

Figure 15. Thin Section of the Base of PAC 2, Sequence II *B* at Mount Union, PA. The base of PAC 2 in Sequence II *B* contains subrounded to subangular quartz grains in an iron-rich, red matrix. The field of view is 1.4 mm horizontally.

the sequence (deposition of PACs 4 and 5 elsewhere). The greater thickness of the sequence at Mount Union can be explained by higher rates of subsidence and proximity to the source of siliciclastics.

<u>Fifth-order Sequence II *C*</u>

Sequence II *C*, the most carbonate-rich sequence in Fourth-order Sequence II, consists of marine carbonate facies at the southern localities, and dominantly non-marine red siltstone and shale facies at Mount Union. Thickness of this sequence is comparable at all three localities (10.5 feet at Pinto, MD, 10 feet at Cedar Cliff, MD, and 12 feet at Mount Union, PA). This ostracod-bearing, carbonate-rich sequence consists of four PACs at the southern localities, where it has been mapped as the Cedar Cliff Limestone Lentil (Hoskins, 1961); only two, carbonate and non-marine siliciclastic PACs could be clearly distinguished at Mount Union (Appendix B).

At all localities, Sequence II *C* is initiated by PAC 2, an ostracod-bearing restricted marine cycle. At the southern localities, this PAC consists of restricted subtidal marine ostracod-rich quartz sandstone (Figure 16 and Table 2), while non-marine (iron-rich red shale) and minor restricted subtidal facies (ostracod-bearing, laminated calcisiltite) constitute the sequence at Mount Union (Table 2). At all three localities, the vertical sequence of PACs in Sequence II *C* exhibits progressive shallowing above the deepest facies at the base of PAC 2. PAC 3 at the southern localities consists of bedded oolitic and pelletal fine calcarenite with ostracods (Figure 17 and Table 2). PAC 4 contains thrombolites, oolites and pellets in calcisiltite. PAC 5 terminates the sequence at the southern localities, consisting of oolites and low intertidal to subtidal thrombolites in

Figure 16. Thin Section of the Base of PAC 2, Sequence II *C* at Cedar Cliff, MD. The base of PAC 2 in Sequence II *C* consists of ostracods in a fine quartz sandstone and calcarenite matrix. Grains are subrounded to subangular in shape. The field of view is 2.9 mm horizontally.

Figure 17. Thin Section of the Base of PAC 3, Sequence II *C* at Cedar Cliff, MD. The base of PAC 3 in Sequence II *C* contains ooids, pellets, and ostracod fragments in fine-grained calcarenite. The field of view is 1.4 mm horizontally.

interbedded shale and laminated limestone (Table 2). In the non-marine facies at Mount Union, PACs consist of restricted lagoonal carbonate or green sandstone overlain by non-marine red siltstone or sandstone caps (Table 2).

Application of the model of an ideal fifth-order sequence (Figure 7) to Sequence II *C* suggests:

1. PAC 1 is missing by hiatus (non-deposition)
2. An eccentricity-enhanced precessional sea-level rise flooded all localities, resulting in deposition of PAC 2.
3. Eccentricity-dampened sea-level rises produced successively shallower PACs 3, 4, and 5 (?) at all localities.

These interpretations are supported by the correlative ostracod-rich quartz arenite and calcarenite at the base of the sequence with subsequent deposition of progressively shallower PACs. Although more subsidence was interpreted at Mount Union than at the southern localities, PAC 5 was not deposited or could not be discriminated. Lateral facies distribution suggests deposition of Sequence II *C* on a gentle slope from dominantly non-marine conditions at Mount Union to restricted-marine environments at Cedar Cliff and Pinto.

Fifth-order Sequence II *D*

Fifth-order Sequence II *D*, the dominantly shaley final sequence of Fourth-order Sequence II, is composed of cycles containing thin, restricted subtidal calcarenite or quartz arenite highstand deposits overlain by supratidal to non-marine shale and siltstone lowstand deposits. Thicknesses of the sequence at Pinto and Mount Union are similar

(14 and 14.5 feet, respectively), while the sequence at Cedar Cliff is not as thick (12 feet). Internally, the southern localities are complete, containing 5 PACs each, while the sequence at the northern locality is composed of 4 PACs (Appendix B).

The first PAC in Sequence II *D* begins with a correlative 1 to 2 foot thick, massive iron-rich red sandstone that is very similar in texture, composition, sorting, and rounding at all localities (Figure 18). At Pinto, PAC 2 is a low-intertidal to subtidal, thin calcarenite bed capped by gray shale (Table 2). Subsequent cycles at Pinto become more shale-rich (Figure 19). At Cedar Cliff, PAC 2 consists of a bioturbated subtidal calcarenite-rich base with a low-intertidal gray to green siltstone cap (Table 2). At Cedar Cliff, PAC 3 highstand deposits contain poorly sorted quartz grains (.1mm average diameter) with silt and clay in bioturbated reduced iron-rich cement capped by green siltstone lowstand deposits. Beds of calcarenite and green siltstone compose the base of PAC 4, which is capped by non-marine red shale (Table 2). PAC 5 contains a thin, iron-rich, non-marine, bioturbated sandstone bed capped by thick, non-marine red shale (Table 2). PACs 2, 3, 4, and 5 in the sequence at Mount Union are composed of red to green sandstone bases with red shale caps; the sandstone becomes greener and less massive and the shale component becomes increasingly thick in successive cycles (Figure 20).

Relative sea-level rise at the beginning of Sequence II *D* initiated the deposition of PAC 1, consisting of an intertidal, two-foot-thick, iron-rich sandstone bed capped by a two-inch-thick gray shale at the southern localities, and capped by non-marine red shale at the northern locality (Appendix B). At the southern localities, gray calcarenite capped by gray shale comprises PAC 2, interpreted as subtidal (Table 2), while this cycle

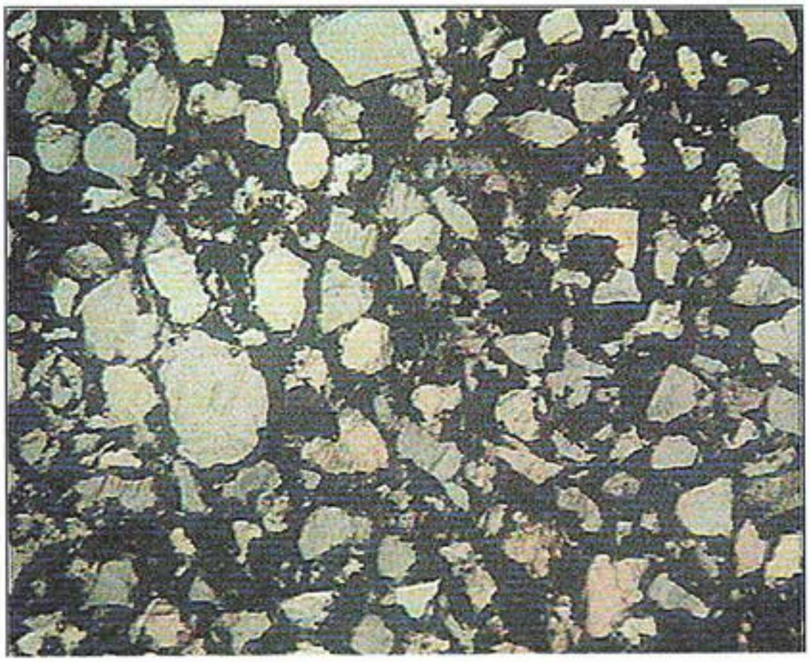

Figure 18. Thin Section of the Base of PAC 1, Sequence II *D* at Pinto, MD. The base of PAC 1 in Sequence II *D* consists of subrounded to subangular quartz grains in an iron-rich, red matrix. The field of view is 1.4 mm horizontally.

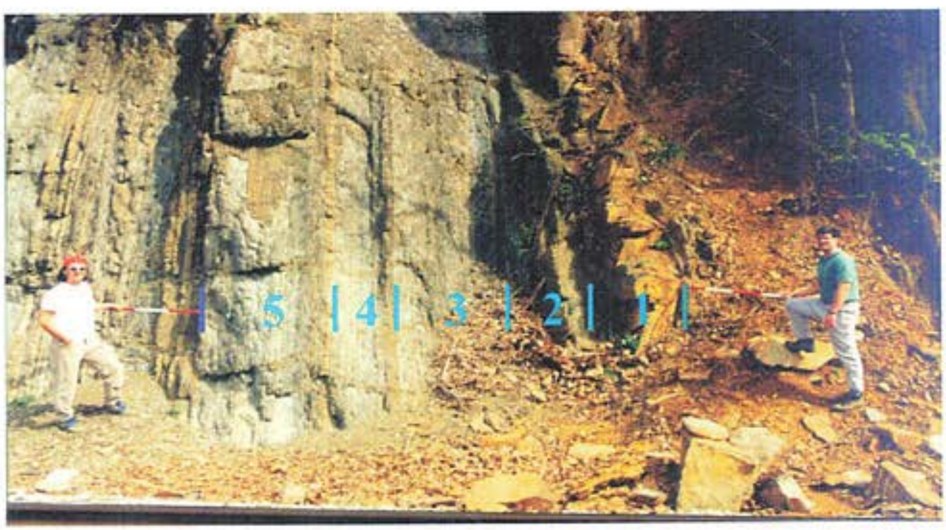

Figure 19. Fifth-order Sequence II *D* at Pinto, MD. Sequence II *D*, bounded by a green line and a dark blue line (fifth-order and fourth-order boundaries, respectively), contains 5 PACs, which are delineated by blue lines. Each PAC in this sequence is composed of gray calcarenite highstand deposits capped by lowstand shale. Measuring sticks are four feet long; stratigraphic up is to the left.

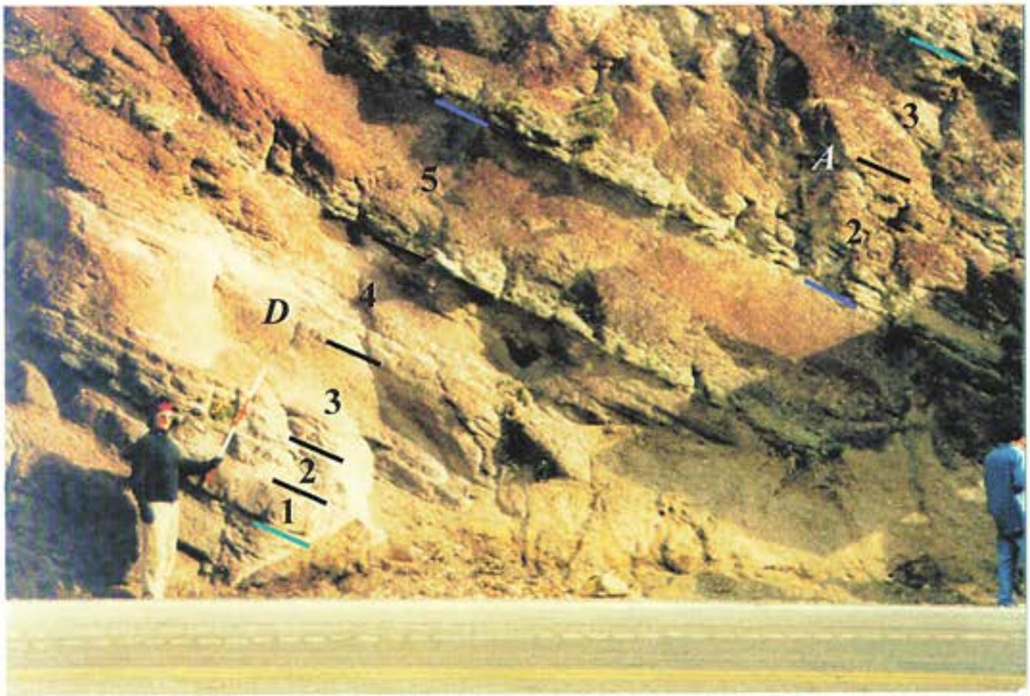

Figure 20. Fifth-order Sequences II *D* and III *A* at Mount Union, PA. Sequence II *D*, bounded by a green line and a blue line (fifth-order and fourth-order boundaries, respectively), contains four PACs, which are delineated by black lines. PACs are composed of red and gray sandstone bases with red shale caps. Sequence III *A*, contains two PACs, which are composed of green calcarenite and red shale. Measuring stick is four feet long; stratigraphic up is toward the top of the page.

consists of red sandstone and shale at the northern locality, reflecting a less marine or non-marine environment. At the southern localities, PAC 3 contains green sandstone, interpreted as low-to mid-intertidal (Table 2), while at Mount Union, this cycle consists of a mid-intertidal highstand, capped by non-marine red shale. PACs 4 and 5 are capped by supratidal red shale at Cedar Cliff (Figures 19 and 21), interpreted to be less marine than at Pinto, where these cycles are capped by intertidal gray shale. The unexpectedly thick sequence at Mount Union can be attributed to relatively high subsidence rates, increasing accommodation space, as interpreted for Sequence II *C* at this locality.

Summary: Fourth-order Sequence II

Determining the position of this fourth-order sequence within the first Wills Creek third-order sequence was accomplished by comparing the patterns of facies change with the expected model (Figures 9 and 12). Although this fourth-order sequence could be either Fourth-order Sequence II or III, relationships of this fourth-order sequence within the third-order sequence and with the subsequent fourth-order sequence indicate that it contains the deepest facies preserved in the third-order sequence, suggesting that it is Fourth-order Sequence II. Using this interpretation, a hiatus of at least 400 Ky occurred at the beginning of the Salina Third-order Supersequence and possibly again at the end of the sequence where Fourth-order Sequence V may also be missing (Figure 12).

Internally, Fourth-order Sequence II is complete at the fifth-order scale, but incomplete at the sixth-order scale. Generally PACs are missing at the bases or tops of fifth-order sequences, especially at Mount Union, the more landward locality. Only precessional sea-level rises associated with eccentricity maximums flooded all localities;

Figure 21. Fifth-order Sequence II *D* and III *A* at Cedar Cliff, MD. Sequence II *D*, bounded by a green line and a dark blue line (fifth-order and fourth-order boundaries, respectively), contains 5 PACs, which are delineated by white lines. PACs consist of limestone or sandstone highstand deposits capped by lowstand gray to red shale. The sequence begins with a correlative, massive iron-rich sandstone, and becomes more shale-rich toward the top. The presence of non-marine red shale in the lowstand deposit of PAC 5, is interpreted to indicate that this locality was slightly shallower than Pinto. PACs in Sequence III *A* consist of fine sandstone and calcarenite highstand deposits capped by lowstand gray to red shales. Measuring sticks are 4 feet long; stratigraphic up is toward the top of the page.

precessional sea-level rises dampened during eccentricity minimums were insufficient to inundate the landward locality.

The paleogeographic interpretation of Fourth-order Sequence II (non-marine at Mount Union, restricted marine at the southern localities) is based on:

1. The facies interpretations of the predominantly sand Sequence II *B* (poorly-sorted, iron-rich, and red at Mount Union; well-sorted and gray at the southern localities).
2. The presence of a paleosol terminating Sequence II *B* at Cedar Cliff, MD; there is no paleosol at that stratigraphic horizon in the section at the most marine locality (Pinto) 5.25 kilometers to the south.
3. The presence of intertidal carbonate facies (high-intertidal laminites and low-intertidal to subtidal thrombolites) at both of the marine southern localities and deposition of oxidized iron-rich, red, non-marine shale in Sequence II *C* at Mount Union, missing in the previous, deeper sequence. (Table 2).
4. In Sequence II *D*, sixth-order lowstand shales change laterally from all non-marine red shale at Mount Union to all gray and green intertidal to supratidal shale at Pinto. At Cedar Cliff, an intermediate locality, red shale is found only in the lowstand deposits of PAC 5, the shallowest PAC in the sequence (Figures 19, 20, and 21).

Fourth-order Sequence III

Fourth-order Sequence III is the second preserved fourth-order sequence of the Salina Supersequence (Figure 11). In contrast to siliciclastic-dominated Sequence II, Fourth-order Sequence III consists of cycles with bedded carbonate bases and shale-rich tops. Laterally, Fourth-order Sequence III contains nearshore marine carbonate and shale at Pinto and Cedar Cliff, and mixed non-marine red shale and restricted marine carbonate deposits at Mount Union. This interpretation is based on observation of lateral facies change in individual PACs. For example, highstand deposits at the southern localities are more carbonate-rich and consistently thicker than the thinner mixed siliciclastic and carbonate, highstand deposits to the north. Furthermore, cycle tops also fit a pattern of being thicker, more iron-rich and red at the northern locality, while the beds are thinner and gray to the south (Appendix B).

Fourth-order Sequence III is similar in thickness at all localities, measuring 32 feet at Mount Union, 32.5 feet at Cedar Cliff, and 33 feet at Pinto (Appendix B). Fourth-order Sequence III is stratigraphically complete, matching the model of a fourth-order sequence (Figure 8) in consisting of four fifth-order sequences. Also consistent with the model (Figure 8), Fifth-order Sequence *B* contains deeper facies than Fifth-order Sequence *A* and Sequences *C* and *D* consist of progressively shallower facies. Although Fourth-order Sequence III is complete at the fifth-order scale, all of its fifth-order sequences are incomplete at the sixth-order scale, especially Sequences C and D.

Fifth-order Sequence III *A*

Representing a relative deepening of facies compared to the shallowing trend (increasing red shale) at the top of Fourth-order Sequence II, Fifth-order Sequence III *A* contains more carbonate and less shale at the southern localities compared to the previous fifth-order sequence. The fifth-order sequence is complete and more marine at the southern localities, but is highly incomplete and thinner at the non-marine Mount Union locality to the north (Appendix B).

At the marine localities, sixth-order cycles consist of fine, calcarenite-rich highstand deposits, interpreted as mid-intertidal deposits (Table 2), capped by high-intertidal gray shales (Figure 21 and 22). The deepest facies in the sequence are the wavy-bedded calcisiltites at the base of PAC 2, at Pinto. Deposition of the sequence at Cedar Cliff was interpreted to be in slightly shallower water than at Pinto, owing to increased quantities of quartz grains in highstand deposits of PACs and the presence of non-marine red shale in this fifth-order sequence (Figure 21). In contrast to the dominantly marine sequence at the southern localities, the non-marine sequence at Mount Union is highly incomplete, consisting of just two cycles (PACs 2 and 3) of green calcarenite and non-marine red shale (Figure 20), interpreted as supratidal facies (Table 2).

The interval at the southern localities compares well with the model of a complete fifth-order sequence (Figure 7), consisting of 5 PACs, of which the first two were produced by enhanced precessional rises. Above the deep facies at the base of PAC 2, highstand deposits of PACs 3, 4, and 5 reflect successive shallowing during a time of decreasing eccentricity. At Pinto, shallowing in PAC 5 produced a thick supratidal shale not present 5.25 kilometers to the north at Cedar Cliff. At Mount Union, the more landward locality, only enhanced precessional rises 2 and 3 flooded the area.

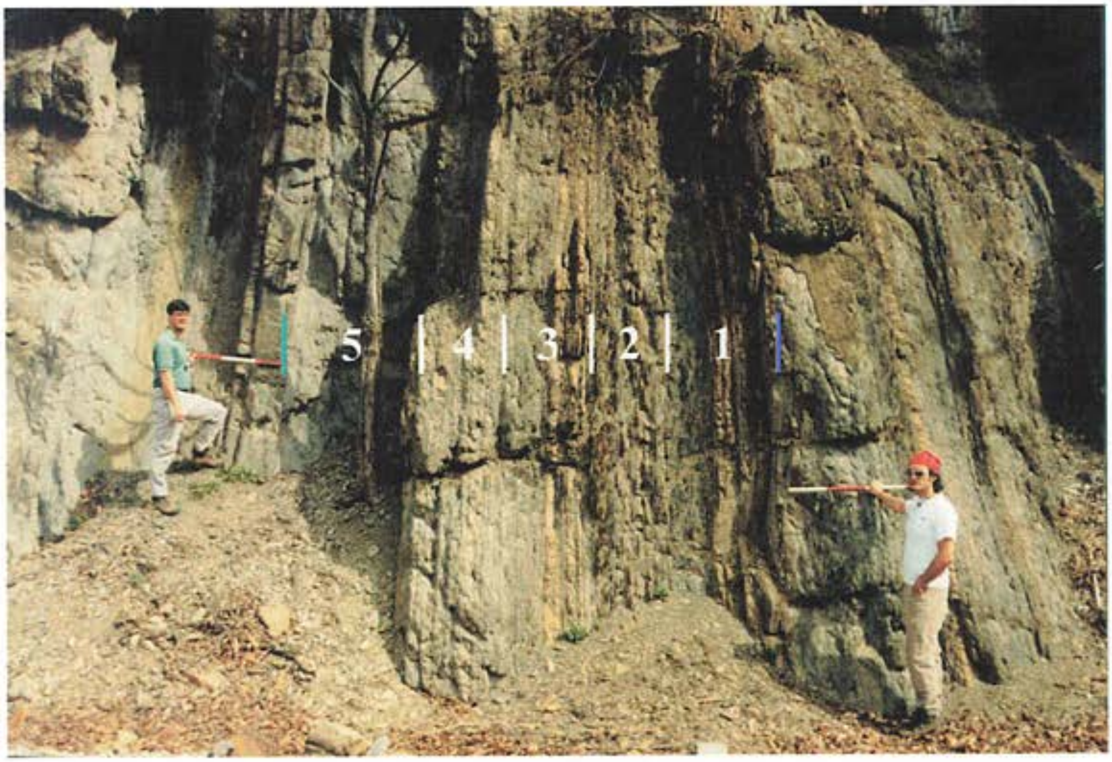

Figure 22. Sequence III *A* at Pinto, Maryland. Sequence III *A*, bounded by a blue line and a green line (fourth-order and fifth-order boundaries, respectively), contains 5 PACs, which are delineated by white lines. PACs in this sequence are delineated by buff to gray carbonate bases capped by shale. The shale at the top of PAC 5 is missing at Cedar Cliff. Measuring sticks are 4 feet long; stratigraphic up is to the left.

Fifth-order Sequence III *B*

Sequence III *B* is initiated at the change from the high-intertidal laminites and supratidal red shale of the previous sequence to massive, subtidal gray calcisiltite and low intertidal gray calcarenite (Appendix B and Table 2). The sequence is thicker toward the north, measuring 7.5 feet at Pinto, 10 feet at Cedar Cliff, and 12.5 feet at Mount Union, PA. Thicknesses at each locality correspond to the completeness of the sequence at those localities; fewer PACs at the most marine locality (Pinto) indicate less accommodation space during the accumulation of this fifth-order sequence.

At the most marine locality (Pinto), sixth-order cycles contain gray, subtidal, fine calcarenite highstand deposits (Figure 23 and Table 2) overlain by low-intertidal, gray shale lowstand tops (Figure 24). At Cedar Cliff, cycles of gray calcarenite and shale become increasingly shale-rich toward the top; the sequence is terminated with a gray shale cycle that is calcareous and bioturbated at the base (Figure 25). PACs 1, 2, and 3 at Mount Union consist of carbonate-rich bases with non-marine, red shale caps (Table 2). The fine calcarenite highstand deposits of PAC 2 (Figure 26) contain less terrigenous silt than the bases of other cycles in the sequence. PAC 4, which terminates the sequence, has a restricted subtidal green siltstone base and a thick red shale top (Table 2).

Comparison of the thickness and completeness of Sequence III *B* at each locality (Appendix B) appears to contradict the expected depositional patterns for marine and non-marine environments, in that the sequence is the thinnest at the most marine locality where one would expect the greatest accommodation space. A possible explanation of the anomalously thin sequence at Pinto is that subsidence decreased at this locality.

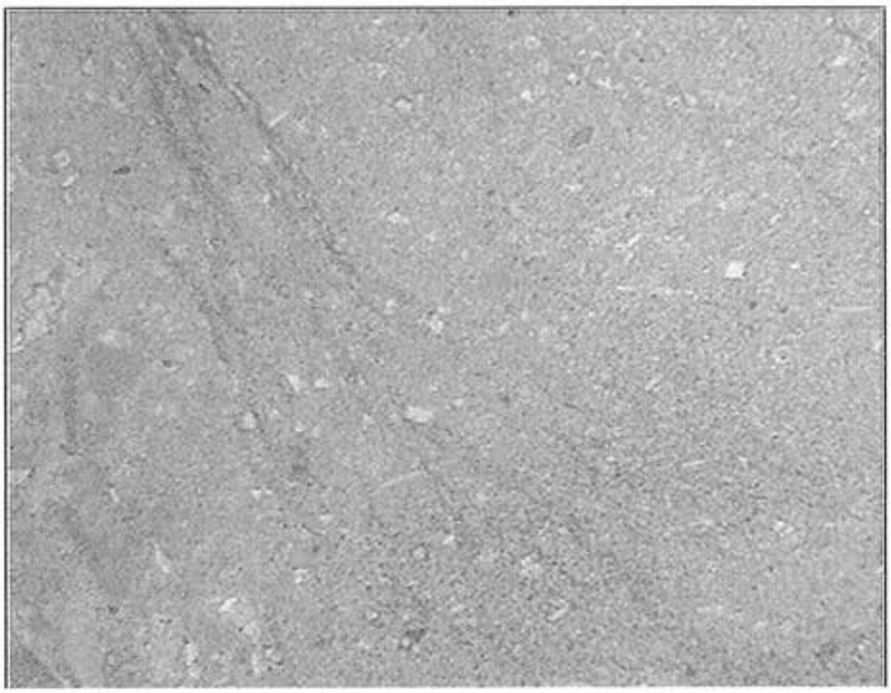

Figure 23. Thin Section of the Base of PAC 2, Sequence III *B* at Pinto, MD.
The base of PAC 2 in Sequence III *B* consists of fine, gray calcarenite. The field of view is 2.9 mm horizontally.

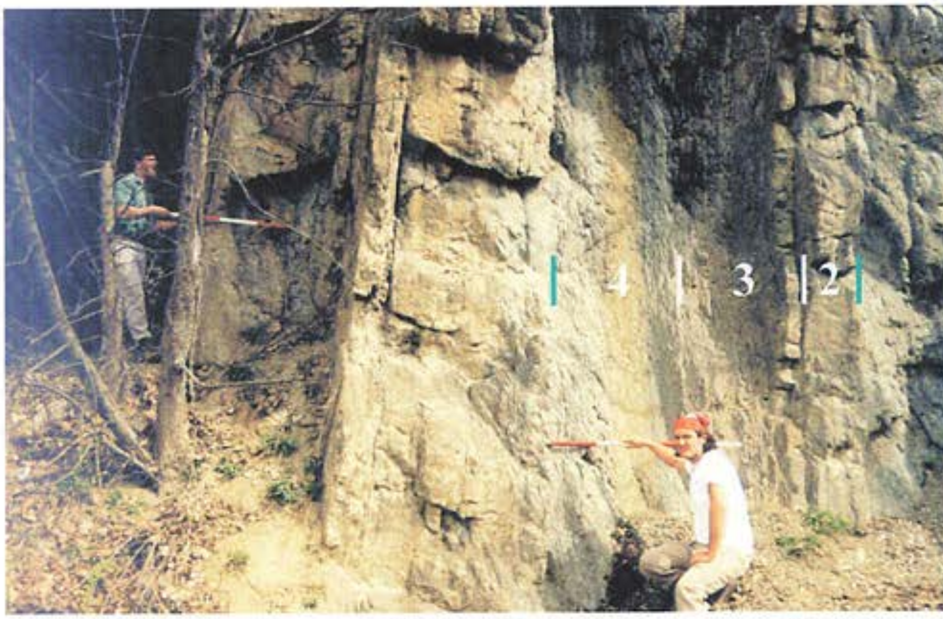

Figure 24. Fifth-order Sequence III *B* at Pinto, MD. Sequence III *B*, bounded by green lines, contains 3 PACs, which are delineated by white lines. PACs in this sequence consist of gray to buff micritic highstand beds overlain by gray to buff shale. Measuring sticks are 4 feet long; stratigraphic up is to the left.

Figure 25. Fifth-order Sequence III *B* at Cedar Cliff, MD. Sequence III *B*, bounded by green lines, contains 4 PACs, which are delineated by white lines. PACs 1, 2, and 3 consist of calcarenite highstand deposits capped by lowstand gray shale; PAC 4 is a gray shale, bioturbated at the base. Measuring sticks are 4 feet long; stratigraphic up is toward the top of the page.

Figure 26. Thin Section of the Base of PAC 2, Sequence III *B* at Mount Union, PA. The base of PAC 1 in Sequence III *B* consists of fine, gray calcarenite. The field of view is 2.9 mm horizontally.

However, similarity in the facies at Pinto and Cedar Cliff suggests similar rates of subsidence throughout the sequence. Also, the similarity of the combined thickness of Sequences III *A* and *B* at all localities suggests constant subsidence. Therefore, the anomalous thickness at Pinto is more likely explained by that locality being topographically higher at the end of Sequence III *A*. This interpretation is supported by the presence of a thick supratidal shale at the top of PAC 5 in Sequence III *A* at Pinto (Table 2), a facies not present at the other two localities (Figure 22). Thus, the precessional sea-level rise initiating PAC 1 of Sequence III *B* was insufficient to inundate Pinto while flooding the other two topographically lower localities (Appendix B). Following flooding of all localities by the second precessional rise, accumulation of the remainder of the sequence occurred under similar environmental and tectonic conditions at all localities.

Fifth-order Sequences III *C* and *D*

Terminating Fourth-order Sequence III are the thin and incomplete Fifth-order Sequences III *C* and III *D* (Figure 27). Sequence III *C*, ranging in thickness from 5 feet to 8 feet, consists of 2 to 3 PACs. Sequence III *D* is even thinner and less complete, ranging in thickness from 2.5 feet to 7 feet and consisting of 1 or 2 PACs (Appendix B). These sequences vary in facies from mid- to high-intertidal carbonates to supratidal shales.

Dampening of the precessional pulse by decreasing eccentricity at the end of the fourth-order and third-order cycles produced thinner and less complete fifth-order sequences at the end of Fourth-order Sequence III at all three localities. At the more

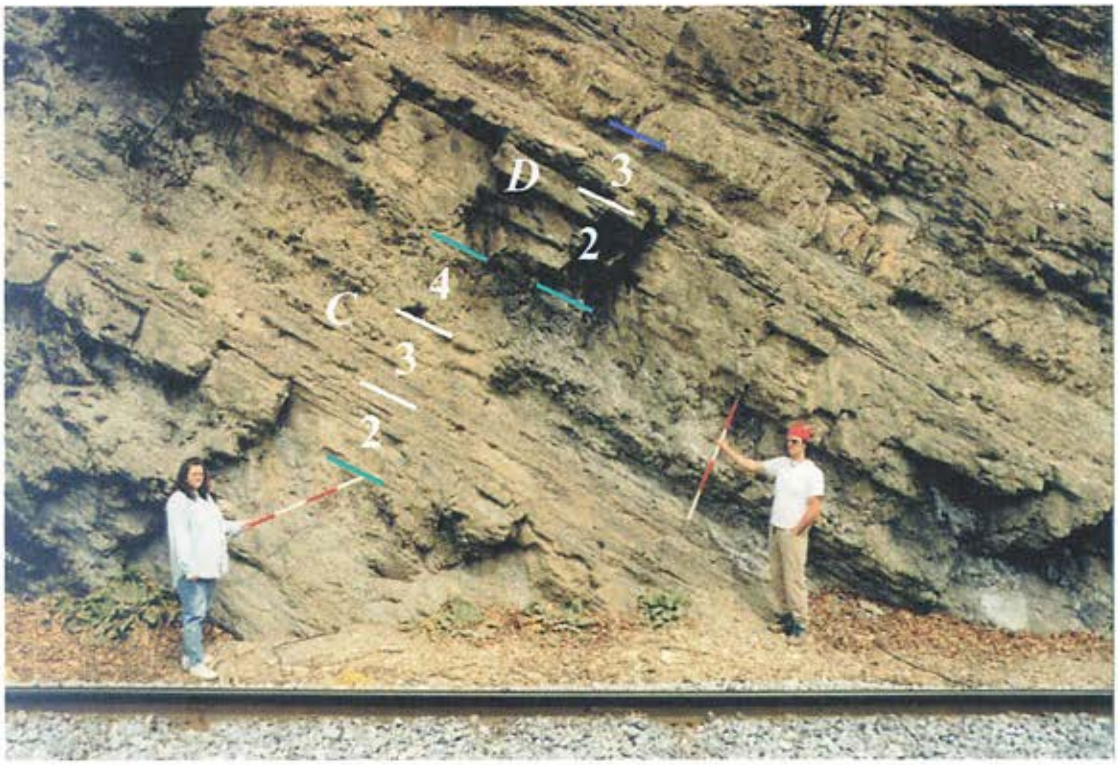

Figure 27. Fifth-order Sequence III *C* and *D* at Cedar Cliff, MD. Sequence III *C*, bounded by green lines, contains 3 PACs, which are delineated by white lines. PACs consist of micrite or calcarenite highstand deposits capped by lowstand gray shale. Sequence III *D*, bounded by a green line and a blue line (fifth-order and fourth-order boundaries, respectively), consists of limestone, mudcracked laminites and gray shale cycles. Measuring sticks are 4 feet long; stratigraphic up is toward the top of the page.

marine localities to the south, both Sequences III *C* and *D* contain more cycles than the same interval at Mount Union (Appendix B).

<u>Summary: Fourth-order Sequence III</u>

The position of this fourth-order sequence within the third-order hierarchy was determined by comparing the patterns of facies change with the expected model (Figures 9 and 12). The lack of a major unconformity at the surface between Fourth-order Sequence II and III was interpreted to indicate that the two sequences were deposited consecutively. Overall, facies in Sequence III are shallower than facies of the previous sequence as expected at a time of long-term eccentricity (Figures 20 and 21). This decrease in accommodation space is also reflected in the higher degree of incompleteness of the four fifth-order sequences, especially Sequences *C* and *D*, of Sequence III (Appendix B). Furthermore, Fourth-order Sequence III is thinner than the previous sequence owing to the decrease in accommodation space. As third-order eccentricity diminished through Fourth-order Sequence III, dampened precessional pulses were insufficient to inundate the localities, resulting in thinner and less complete sequences.

Study Interval Cyclicity: Summary

The study interval, consisting of two fourth-order sequences, was interpreted to contain the second and third fourth-order sequences in Third-order Sequence A of the Salina Supersequence (Figures 12 and 28). These fourth-order sequences are complete at the fifth-order scale, each consisting of four fifth-order sequences. However, each fifth-order sequence is incomplete at the sixth-order scale, by hiatus at the top or bottom of the sequences. The sequences contain more marine facies at the southern localities, with

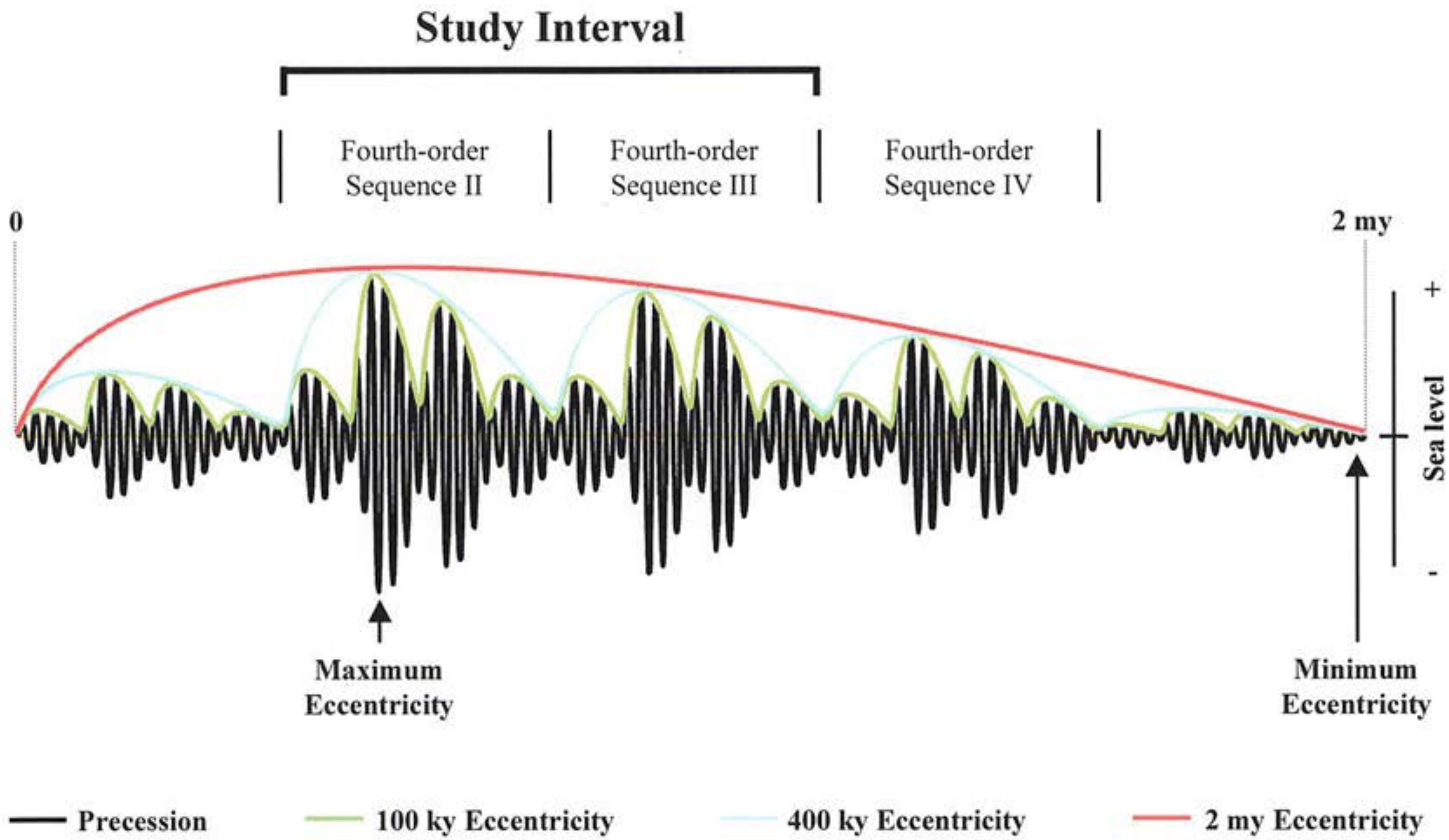

Figure 28. Position of Study Interval within 2 my Third-order Sequence A. The study interval consists of Fourth-order Sequences II and III, the first two preserved sequences within the 2 my duration Third-order Sequence A (see also Figure 12). Fourth-order Sequence II, at the base of the Salina Supersequence rests unconformably on the Mifflintown Supersequence.

Cedar Cliff, MD being slightly more onshore than Pinto, MD; non-marine facies dominate at Mount Union, PA. At the most landward locality (Mount Union), most fifth-order sequences are less complete that at the southern localities. Similar thicknesses for the study interval at all localities suggest that the subsidence rate remained constant for 800 ky, the duration of the two fourth-order sequences. Thus, incompleteness is interpreted as resulting from variations in amplitude of sea-level fluctuations, primarily as a function of eccentricity-modulation of the precessional signal.

CHAPTER 4

BASIN DYNAMICS

Characteristics of Fourth-order Sequences

The study interval comprises two fourth-order sequences (Sequences II and III) in Third-order Sequence A of the 10 my Salina Supersequence (Figures 10 and 11). In the study area (Central Pennsylvania and Western Maryland) Fourth-order Sequence I is missing by hiatus at the unconformity with the Mifflintown Supersequence below. Total thickness of the study interval at each locality is relatively constant, ranging from 76.5 feet at Cedar Cliff, MD to 81 feet at Pinto, MD, and 83 feet at Mount Union, PA. Sequence II is approximately 50 percent thicker (averaging 47.5 feet) than Sequence III (averaging 32.5 feet) and contains a greater diversity of facies, including the most marine facies in the study interval. The study interval at each locality fits the pattern of an ideal fourth-order sequence, containing four fifth-order sequences composed of from 1 to 5 cycles (PACs). Fourth-order sequences have characteristic patterns of facies change, with sandstone or carbonate-dominated bases and increasingly shallow, shale-rich facies toward the top of each sequence.

Sequence II, the first preserved fourth-order sequence in the Salina Supersequence, contains unique facies mapped traditionally as the Williamsport Sandstone and the Cedar Cliff Limestone Lentil (Hoskins, 1961). These unique shallow marine facies grade into non-marine red sandstone and shale facies to the north at Mount Union. Thickness of the sequence ranges from 44 feet at Cedar Cliff to 51 feet at Mount Union. At all localities, the fourth-order sequence consists of the requisite four fifth-order sequences. Although the sequence is thickest at Mount Union, it contains fewer sixth-order cycles than at the southern localities (Appendix B1).

Fourth-order Sequence III consists of carbonate and shale facies that are typical of the rest of the Lower Wills Creek Formation. This fourth-order sequence is significantly thinner and more uniform in thickness than Fourth-order Sequence II, measuring 32 feet at Mount Union, PA, 32.5 feet at Cedar Cliff, MD, and 33 feet at Pinto, MD. Similar to Sequence II, Sequence III is complete at the fifth-order scale, but Sequence III is more incomplete at the sixth-order scale, especially at the non-marine locality of Mount Union, and in the last two fifth-order sequences at all localities (Appendix B1).

Stratigraphic Processes

Stratigraphic accumulation of the study interval was influenced by eustatic sea level change, subsidence, and paleogeographic position of the localities. The primary factor in cycle production was eustasy, predominantly controlled by precession, and modulated by three periods of eccentricity (100 ky short eccentricity, 400 ky long eccentricity, and 2 my eccentricity). Subsidence and paleogeographic position affected thickness of the section and the types of sediments deposited.

<u>Eustasy</u>

Precession was the principal cycle-producing mechanism during deposition of the study interval. Precessional cycles (sixth-order cycles or PACs) are sharply bounded 20 ky packages of sandstone and carbonate highstand deposits overlain by shaley lowstand deposits. These cycles average 2.4 feet in thickness at the marine localities and 3.8 feet at Mount Union. This difference in average thickness may be a function of greater subsidence rates at Mount Union or it may mean that PAC boundaries are obscured in these non-marine facies. The fact that cycles at Mount Union are usually more shaley than cycles at the southern localities suggests that the original thickness differential was even greater than the current differential. Therefore, subsidence rates were probably greater at Mount Union.

Modulation of the precessional signal by short eccentricity (100 ky) bundled PACs into asymmetric fifth-order sequences, which average 10 feet in thickness. During periods of high eccentricity, precessional sea-level changes were enhanced, producing a major facies change at the beginning of a fifth-order sequence and another significant facies change to the second cycle in the sequence. Conversely, during periods of low eccentricity, dampened precessional sea-level rises and falls generated successively shallower PACs in the upper portion of the fifth-order sequence (Figure 7).

Precessional sea-level fluctuations were also enhanced and dampened by eccentricity at two larger scales, a 400 ky cycle and possibly a 2 my cycle (Figures 8 and 9). The 400 ky eccentricity cycle bundled fifth-order sequences into fourth-order sequences, each of which has a predictable symmetry reflecting long-term periods of high and low eccentricity (Figure 8). While the basic asymmetry of each fifth-order sequence was maintained (Figure 7), the amplitude of sea-level fluctuations was influenced (enhanced or dampened), resulting in greater facies changes and deeper facies in the first and second fifth-order sequences. Similarly, third-order sequences are possibly the result of the 2 my eccentricity cycle which bundled fourth-order sequences into large-scale, generally shallowing-upward sequences (Figure 9).

Modulation of the precessional pulse by eccentricity also affected the completeness of the sequences. During periods of maximum eccentricity (at any scale) cycles were more likely to be preserved, because accommodation space was greater owing to enhanced precessional sea-level rises (Figure 9). During periods of minimal eccentricity, cycles were often not deposited because dampened precessional sea-level rises were insufficient to flood the nearshore and/or non-marine localities (e.g., Sequences III *C* and *D* in Appendix B1).

Subsidence

Given adequate supply of sediment, subsidence is the principal control of stratigraphic thickness (Anderson, et al., 1986). For the study interval, supply of sediment was sufficient to fill all accommodation space; essentially all cycles shallow upward to sea-level facies. Therefore, vertical and lateral variations in thickness between sequences and among localities can be attributed to differences in subsidence. For the study interval as a whole, average subsidence rates were similar at all three localities, as evidenced by similar thicknesses (81 feet at Pinto, 76.5 feet at Cedar Cliff, and 83 feet at Mount Union) and similar facies (Appendix B1). Vertically, Sequence III is thinner and less complete than Sequence II at all localities, indicating decreased subsidence rates during the accumulation of Sequence III. An average thickness of 32 feet for Sequence III, compared to an average thickness of 48 feet for Sequence II, suggests that the subsidence rate for Sequence III was approximately two-thirds of the rate for Sequence II.

However, differential compaction of the more shaley Sequence III needs to be considered because shale compacts much more than carbonate during lithification. If compaction occurred early, as dewatering of clays, during accumulation of a single shaley PAC, then original PAC thicknesses would have been comparable to current thicknesses, and thickness would be proportional to subsidence. If, on the other hand, compaction occurred later, after burial of a sequence of PACs, then original thicknesses of shaley PACs were substantially greater that current thicknesses. In that case, greater subsidence rates would be required to produce accommodation space for the accumulation of twice as much intertidal and supratidal shale. Thus, if compaction occurred after the study interval was buried, rates of subsidence would not be proportional to current thickness. In that case, estimates of subsidence rates for Sequence III would be too low.

Therefore, the issue of differences in subsidence rates between Sequence II and Sequence III depends on the timing of compaction and the amount of differential compaction. Although evidence of timing of compaction is sparse, a study by Teodorovich and Chernov (1968) suggests that significant (approximately 26 percent) loss of porosity and therefore loss of volume occurs in clays within 8 to 10 meters of burial. Whether this reduction can occur within a meter or less of accumulation, and therefore within the time of accumulation of a single PAC, has not been determined. Lacking a comprehensive study of the timing of compaction in the context of an allocyclic framework, the difference in thickness between Sequence II and Sequence III is interpreted as resulting from decreasing subsidence possibly combined with dampened sea-level rises caused by the long-term (2 my) eccentricity cycle.

Paleogeographic Position

The relative paleogeographic position of each locality along the shoreline affected the facies characteristics of cycles and sequences. Persistently shallower facies at Mount Union, PA indicate that this locality was situated more onshore than the southern localities (Figure 29). At Mount Union, the most non-marine locality, proximity to the Appalachian highlands to the east increased the siliciclastic content of Sequence II *B*, *C*, and *D* and Sequence III *A* relative to the southern localities (Appendix B1). Furthermore, the presence of sandstone and red shale in Sequence III *B* at Mount Union can also be interpreted as evidence of closer proximity to siliciclastic sources in relation to the carbonate and gray shale-rich Sequence II *B* at Pinto, MD. Along the muddy shoreline at the eastern edge of the Appalachian Basin, precessional rises inundated the localities, generating temporary times of clear water carbonate deposition, during precessional highstands. Although the southern localities were more offshore relative to Mount Union, the gentle slope of the basin edge coupled with low-amplitude sea-level rises restricted water depth to a few meters even during deposition of the first and second (maximum water depth) cycles within each fourth-order sequence.

Thus, this study has discriminated the contributions of orbitally forced eustasy, subsidence, and paleogeographic position in the accumulation of two Lower Silurian fourth-order sequences, encompassing 800 ky. While subsidence and paleogeographic position affected total thickness and general composition of facies within the study

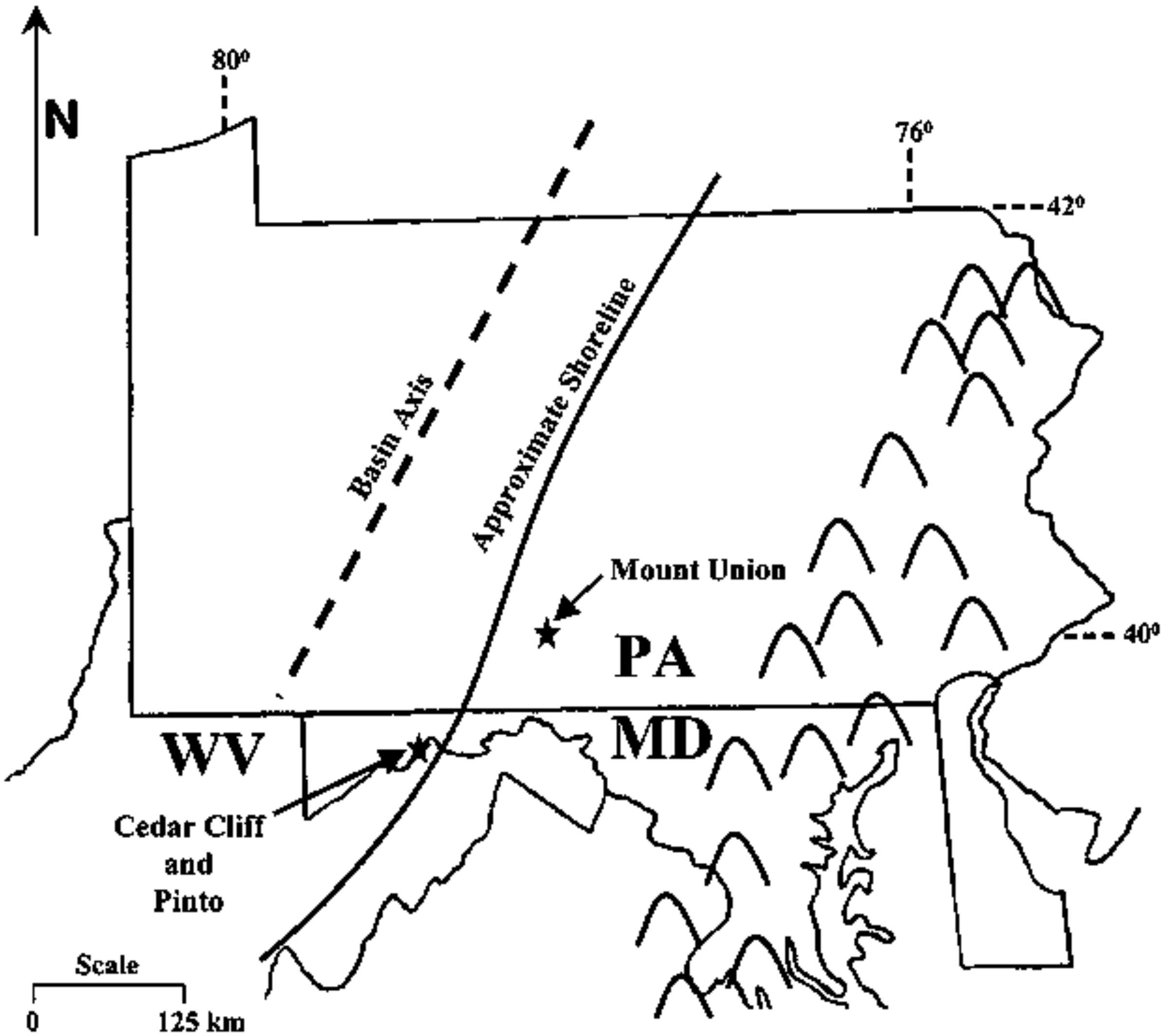

Figure 29. Late Silurian Paleogeography. Study localities are marked by stars. The northern locality (Mount Union, PA) is closer to siliciclastic sources to the east. Shoreline is an approximation of maximum and minimum sea levels.

interval, the principal mechanism responsible for hierarchic cyclicity is the precessional signal modulated by eccentricity at two (possibly three) scales. The existence of hierarchic cyclic patterns matching the predictions of the Milankovitch model during a time of minimal to nonexistent continental glaciation (Bambach et al., 1981 and Chumakov, 1984) suggests that this process-determined model may have general application throughout the stratigraphic record.

REFERENCES CITED

Anderson, E.J., Goodwin, P.W., and Sobieski, T.H., 1984, Episodic accumulation and the origin of formation boundaries in the Helderberg Group of New York State: Geology, v. 12, p. 120-123.

Bambach, R.K., Scotese, C.R., Ziegler, A.M., 1980, Before Pangea: The geographies of the Paleozoic world: *in* Skinner, B.J. (ed) Climates Past and Present. 1981, 135 p.

Bassinot, F.C., Labeyrie, L.D., Vincent, E., Quidelleur, X., Shackleton, N.J., and Lancelot, Y., 1994, The astronomical theory of climate and the ice age of the Brunhes-Matuyama magnetic reversal: Earth and Planetary Letters, v. 126, p. 91-108.

Bayer, U., and M[c]Ghee, G. R., Jr., 1986, Cyclic patterns in the Paleozoic and Mesozoic: implications for time scale calibrations: Paleoceanography, v. 1, p. 383-402.

Berg, T.M., McInerney, M.K., Way, J.H., MacLachlan, D.B., 1986, Stratigraphic Correlation Chart of Pennsylvania: Commonwealth of Pennsylvania Department of Environmental Resources, Office of Resources Management, Bureau of Topographic and Geologic Survey, General Geology Report n. 75, 1 sheet.

Berger, A., 1988, Milankovitch theory and climate: Reviews of Geophysics, v. 26, p. 624-657.

Berger, A., 1989, Pleistocene climatic variability at astronomical frequencies: Quaternary International, v. 2, p. 1-14.

Berger, A., and Loutre, M.F., 1992, Astronomical solutions for paleoclimate studies over the last 3 million years: Earth and Planetary Letters, v. 111, p. 369-382.

Brown, S.M., 1999, Correlation of a hierarchy of cycles forced by eccentricity and precession: Middle Wills Creek Formation, Central Appalachian Basin: Unpublished Master's Thesis, Temple University, Philadelphia, PA.

Chadwick, W., 1993, Correlation of Milankovitch-Band cyclicity in the peritidal carbonates of the Tonoloway Formation, Central Pennsylvania and Western Maryland: Unpublished Master's Thesis, Temple University, Philadelphia, PA.

Chumakov, N.M., 1984, The principal glacial events of the past and their geologic significance: International Geology Review, v. 26, p. 869-888.

DeBoer, P.L., and Smith, D.G., 1994, Orbital forcing and cyclic sequences: Special Publication of International Association of Sedimentologists, v. 19, p. 1-14.

Fischer, A.G., and Bottjer, D.J., 1991, Orbital forcing and sedimentary sequences: Journal of Sedimentary Petrology, v. 7, p. 1063-1069.

Goldhammer, R.K., Dunn, P.A., Hardie, L.A., 1987, High frequency glacio-eustatic sealevel oscillations with Milankovitch characteristics recorded in Middle Triassic platform carbonates in Northern Italy: American Journal of Science, v. 287, p. 853-892.

Goldhammer, R.K., Dunn, P.A., Hardie, L.A., 1990, Depositional cycles, composite sea-level changes, cycle stacking patterns, and the hierarchy of stratigraphic forcing: Examples from Alpine Triassic platform carbonates: Geological Society of America Bulletin, v. 102, p. 535-562.

Goldhammer, R.K., Oswald, E.J., and Dunn, P.A., 1994, High-frequency, glacio-eustatic cyclicity in the Middle Pennsylvanian of Paradox Basin: An evaluation of Milankovitch forcing: Special Publication of International Association of Sedimentologists, v. 19, p. 243-283.

Goodman, W.M., and Brett, C.E., 1994, Roles of eustasy and tectonics in development of Silurian stratigraphic architecture of the Appalachian Foreland Basin: Society for Sedimentary Geology, v. 4, p. 147-169.

Goodwin, P.W., and Anderson, E.J., 1985, Punctuated Aggradational Cycles: A general hypothesis of episodic stratigraphic accumulation: Journal of Geology, v. 93, n. 5, p. 515-533.

Goodwin, P.W., Anderson, E.J., Goodman, W.M., and Saraka, L.J., 1986, Punctuated Aggradational Cycles: Implications for stratigraphic analysis: Paleoceanography, v. 1, n. 4, p. 417-429.

Goodwin, P.W., and Anderson, E.J., 1988, Episodic development of Helderbergian Paleogeography, New York State, Appalachian Basin: *in* McMillan, N.J., Embry, A.F. & Glass, D.J. (eds) Devonian of the World. Second International Symposium on the Devonian System, Canadian Society of Petroleum Geologists, p. 553-568.

Goodwin, P.W., and Anderson, E.J., 1997, Stratigraphic incompleteness: Milankovitch in the Manlius at the margin: Guidebook for the 69th Annual Meeting, New York State Geological Assoc., p. 237-249.

Haq, B.U., Hardenbol, J., and Vail, P.R., 1987, Chronology of fluctuating sea levels since the Triassic: Science, v. 235, p. 1156-1166.

Haq, B.U., and Van Eysinga, F.W.B., 1998, Geological Time Table: 5edition, Elsevier Press, New York.

Harland, W.B., Cox, A.V., Llewellyn, P.G., Pickton, C.A.G., Smith, A.G., and Walters, R., 1982, A Geologic Time Scale. Cambridge University Press, Cambridge, United Kingdom, 131 p.

Hoskins, D.M., 1961, Stratigraphy and paleontology of the Bloomsburg Formation of Pennsylvania and adjacent states: Pennsylvania Topographic and Geological Survey Bulletin, v. G36, p. 48-52 and 61.

Imbrie, J., and Imbrie, J.Z., 1980, Modeling the climatic response to orbital variations: Science, v. 207, p. 943-953.

Lacey, J.E., 1960, Cyclic sedimentation in the Silurian Wills Creek and Tonoloway Formations at Mount Union, Pa.: unpublished M.S. Thesis-University of Pittsburgh.

Mauriello, D.J., Goodwin, P.W., and Anderson, E.J., 1994, Milankovitch control on the stratigraphic positioning of iron beds within the Clinton Group: Geological Society of America, Program with Abstracts, v. 26, n. 3, p. 53.

Mauriello, D.J., and Ketterer, M.W., 1993, Correlation of hierarchical Upper Silurian stacking patterns generated by Milankovitch orbital forcing: Geological Society of America, Program with Abstracts, v.25, n. 2, p. 59.

Mesolella, K.J., Matthews, R.K., Broecker, W.S., and Thurber, D.L., 1969, The astronomical theory of climatic change: Barbados data. Journal of Geology, v. 77, p. 250-274.

Milankovitch, M., 1941, Kanon der erdbestrahlung und seine anwendung auf das eiszeitenproblem:* Special Publication of the Royal Academy of Serbia, Belgrade, v. 132, 633 p. (English translation U.S. Department of Commerce). *Canon of insolation and the ice-age problem, Belgrade Serbian Academy of Science.

Mitchum, R.M., Vail, P.R., Thompson, S., III, 1977, Seismic stratigraphy and global changes of sea level, Part 2: The depositional sequence as a basic unit for stratigraphic analysis: *In* Payton, C.E. ed., Seismic Stratigraphy-Applications to Hydrocarbon Exploration: American Association of Petroleum Geologists Memoir, v. 26, p. 53-62.

Mitchum, R.M., Van Wagoner, J.C., 1991, High-frequency sequences and their stacking patterns: sequence-stratigraphic evidence of high-frequency eustatic cycles: Sedimentary Geology, v. 70, p. 131-160.

Peltier, W.R., and Jiang, Xianhua, 1994, The precession constant of the Earth: Variations through the ice age: Geophysical Research Letters, v. 21, p. 2299-2302.

Rickard, L.V., 1962, Late Cayugan (Upper Silurian) and Helderbergian (Lower Devonian) stratigraphy in New York: New York Museum Science Service Bulletin 386, 157 p.

Shackleton, N.J., Berger, A., Peltier, W.R., 1990, An alternative astronomical calibration of the lower Pleistocene timescale based on ODP Site 677: Transactions of the Royal Society of Edinburgh, v. 81, p. 251-261.

Shelton, Susan, 1995, The Williamsport Sandstone: Precession and eccentricity forced cyclicity in the Upper Silurian strata of Central Pennsylvania, Western Maryland, and Northeastern West Virginia: Unpublished Master's Thesis, Temple University, Philadelphia, PA.

Smith, Langhorne B., and Anderson, E. J., 1992, Late Silurian Milankovitch hierarchal cyclicity: Geological Society of America, Program with Abstracts, v. 24, n. 3, p. 48.

Stose, G.W., 1912, U.S. Geological Survey Atlas, Pawpaw-Hancock folio (No. 179) p. 1-24.

Strasser, A., 1994, Milankovitch cyclicity and high-resolution sequence stratigraphy in lagoonal-peritidal carbonates (Upper Tithonian-Lower Berriasian, French Jura Mountains): Special Publication of the International Association of Sedimentologists, v. 19, p. 285-301.

Swartz, C.K., 1923, Geologic relations and geographic distribution of the Silurian strata of Maryland: Maryland Geologic Survey, Silurian Volume, p. 40-211.

Swartz, F.M., 1934, Silurian section near Mount Union, Central Pennsylvania: Bulletin of the Geological Society of America, v. 45, p. 81-134.

Teodorovich, G.I., and Chernov, A.A., 1968, Character of changes with depth in productive deposits of Apsheron oil-gas-bearing region. Soviet Geology, v. 4, p. 83-93.

Tourek, T.J., 1970, The depositional environments and sediment accumulation models for the Upper Silurian Wills Creek shale and Tonoloway limestone, Central Appalachians: unpublished Ph.D. Thesis-Johns Hopkins University.

Vail, P.R, Mitchum, R.M., and Thompson, S. III, 1977, Seismic stratigraphy and global change of sea-level, Part 3: relative changes of sea-level from coastal onlap: *in* Payton, C.E. (ed), Seismic Stratigraphy-Applications to Hydrocarbon Exploration: American Association of Petroleum Geologists Memoir, v. 26, p. 63-81.

Zeliznak, C.K., Brown, S.M., Goodwin, P.W., and Anderson, E.J., 1997, Facies patterns that define Wills Creek 5th and 6th order cycles: Geological Society of America, Program with Abstracts, v. 29, n. 1, p. 10.

APPENDIX A1. LOWER WILLS CREEK FORMATION AT MOUNT UNION, PENNSYLVANIA.

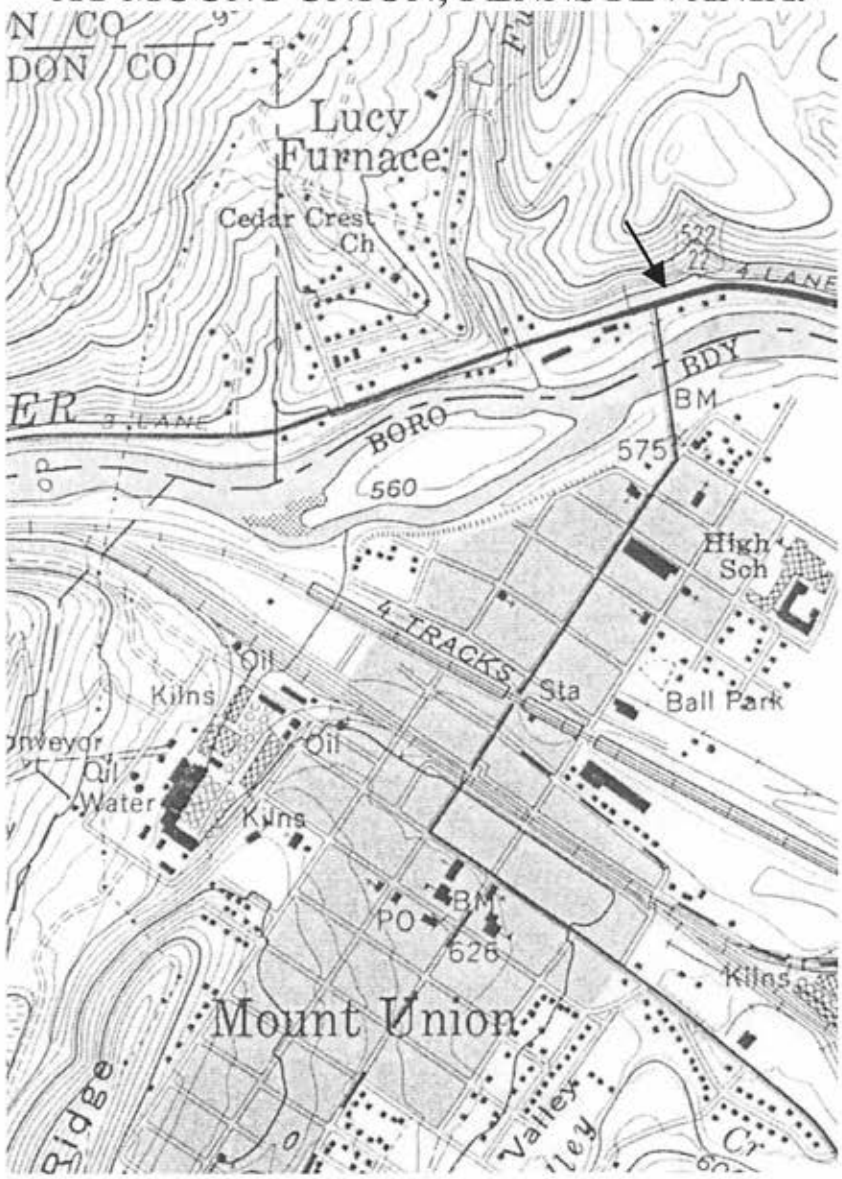

0.2 mile

Scale

Location of Section at Mount Union, PA. The section at Mount Union is located on the Mount Union, PA quadrangle at coordinates 40^{0} 23' 41" N Latitude, 77^{0} 52' 45" W Longitude. The outcrop is located along a roadcut for U.S. Routes 522 and 22 on the north side of the highway across the Juniata River from the town of Mount Union, Pennsylvania. The study section is located with an arrow.

APPENDIX A2. LOWER WILLS CREEK FORMATION AT CEDAR CLIFF, MARYLAND.

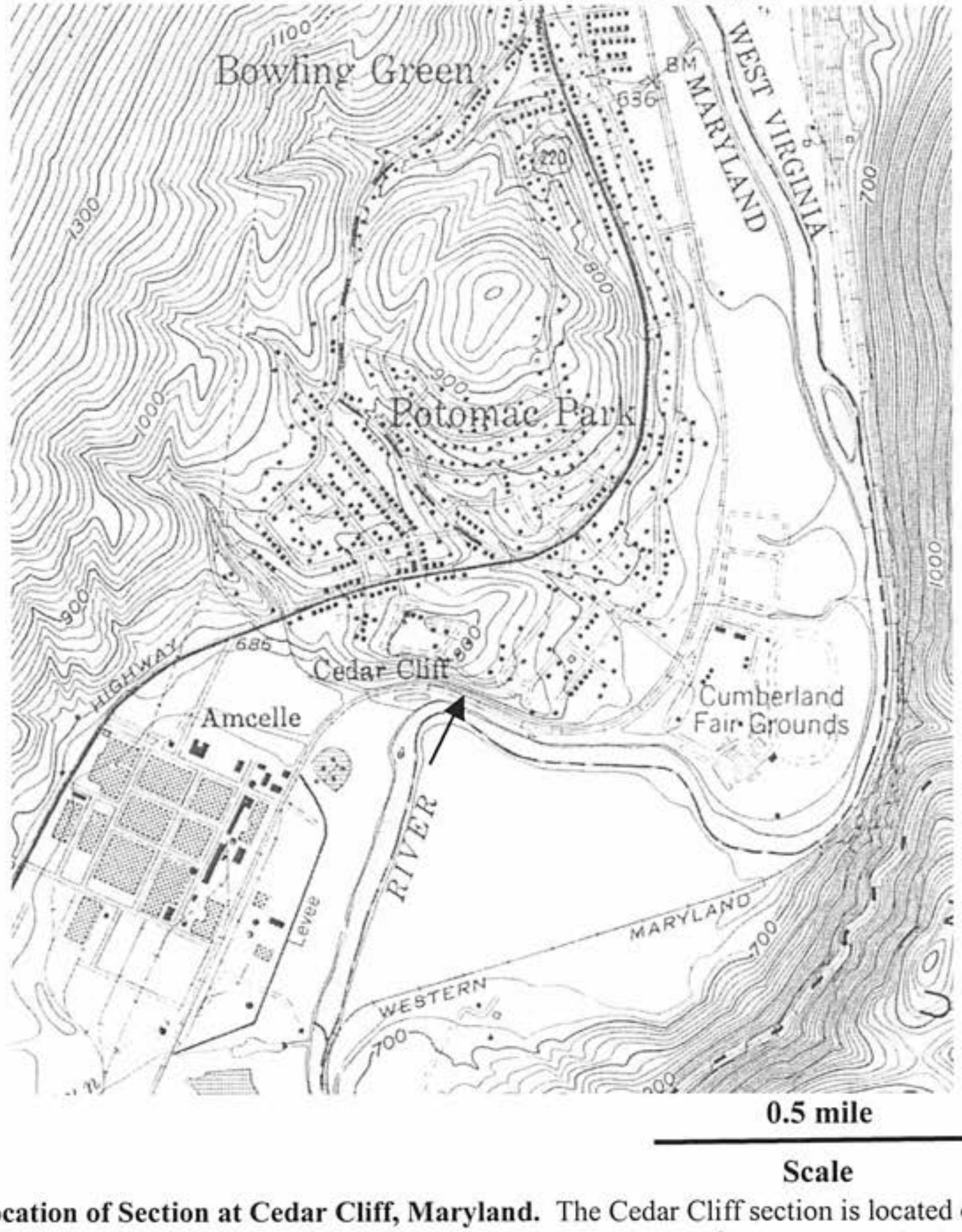

Location of Section at Cedar Cliff, Maryland. The Cedar Cliff section is located on the Cresaptown, MD quadrangle at coordinates 39^0 36' 31" N Latitude, 78^0 48' 30" W Longitude. The outcrop is in Cedar Cliff, Maryland, 5 miles south of Cumberland, Maryland along the Conrail tracks adjacent to the Juniata River. Access to the tracks is from the end of the road leading to the Cumberland Fair Grounds, 0.5 miles east of Route 220. The study section is located with an arrow.

APPENDIX A3. LOWER WILLS CREEK FORMATION AT PINTO, MARYLAND.

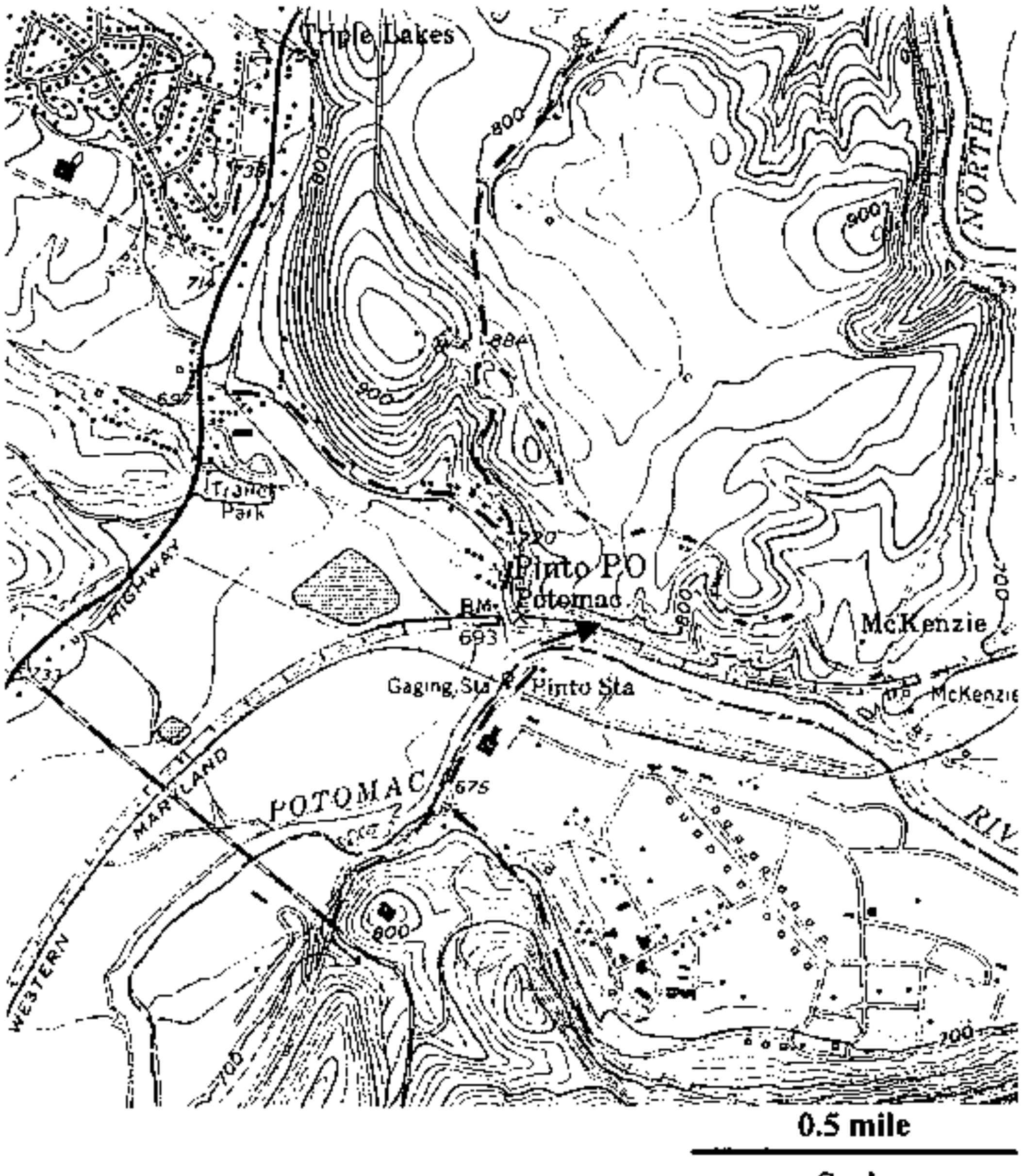

Location of Section at Pinto, Maryland. The section at Pinto is located on the Cresaptown, MD Quadrangle, at coordinates 39^{0} 34' 02"N Latitude, 78^{0} 50' 12"W Longitude. The outcrop is in the town of Pinto, Maryland, 7.4 miles south of Cumberland, Maryland, along the Conrail tracks adjacent to the Juniata River. Access to the tracks is from the end of Pinto Road, 0.7 miles east of Route 220. The study section is located with an arrow.

APPENDIX B1. CORRELATION OF STUDY INTERVAL

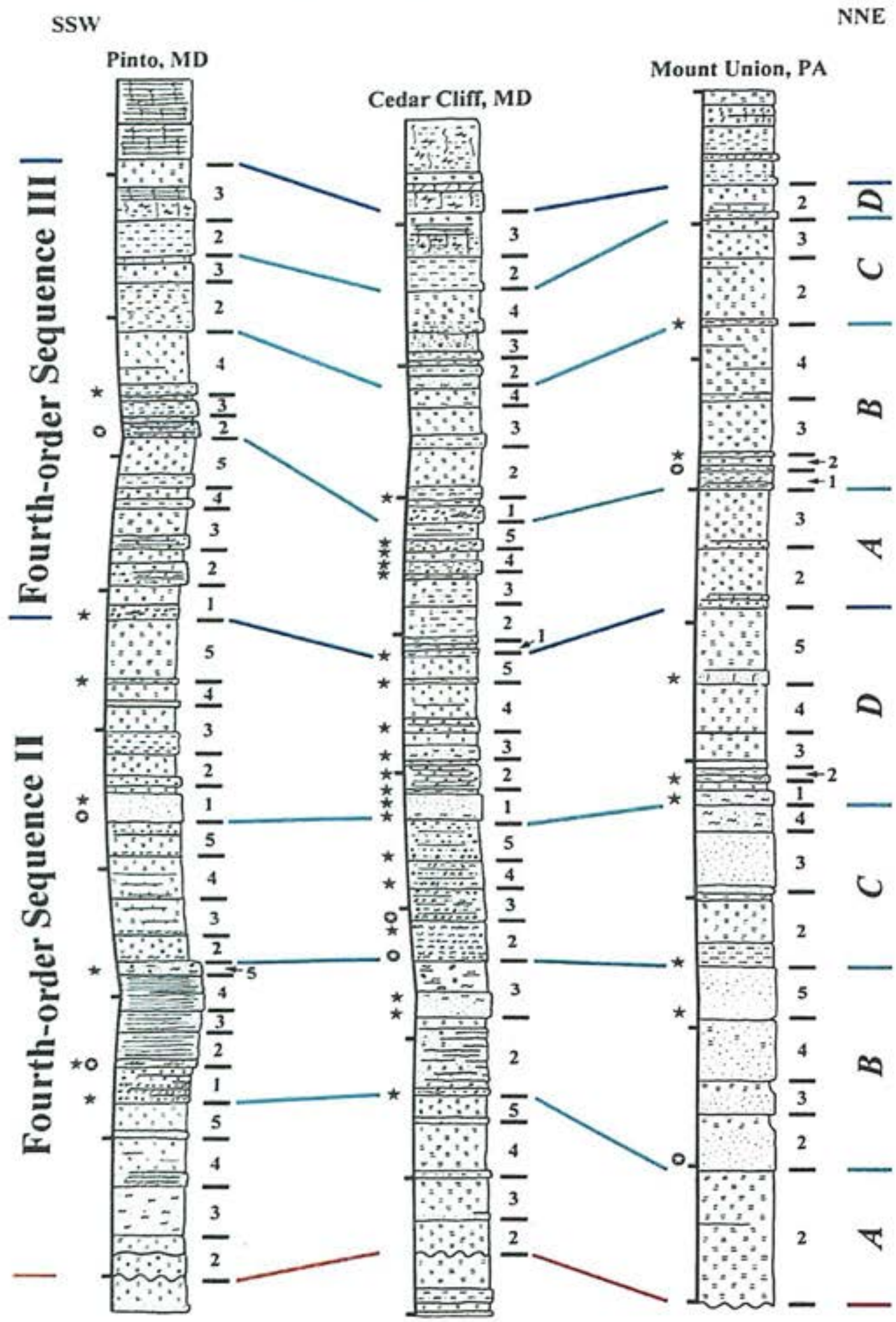

Correlation of Study Interval. Correlation of two fourth-order sequences using the Genetic Hierarchy of Allocycles of Goodwin and Anderson (1997). The Mifflintown/Salina Supersequence unconformity (third-order boundary) is indicated by the red line. Fourth-order sequences are bounded by blue lines. Fifth-order sequences, indicated by italicized capital letters, are bounded by green lines. PAC (sixth-order) boundaries are indicated by black lines right of each column. Samples were taken from stratigraphic horizons marked with a ★; samples pictured as thin-sections in text are marked by a O. Black lines on the left edge of each column are ten-foot marks. Symbol key is in Appendix B2.